

Modulation of superlattice band structure via δ doping

G. Ihm, S. K. Noh, J. I. Lee, and J.-S. Hwang

Quantum Physics Laboratory, Korea Standards Research Institute, Taejon 305-606, Korea

T. W. Kim

Department of Physics, Kwangwoon University, Seoul 139-050, Korea

(Received 15 April 1991)

A way of modulating superlattice band structure is presented utilizing a δ -doping technique. Enormous changes in the electronic states of a superlattice can be made by introducing spatially localized defects with a periodic array in the well layers as well as in the barrier layers of a superlattice. Along with an analytic energy dispersion relation, it is shown that the creation of a band or the annihilation of a given band and the control on the miniband gap, band positions, and their widths are now possible by adjusting the weight and the position of the inserted defects.

Recently, Beltram and Capasso¹ have shown that the periodic introduction of deep levels within the barrier region of semiconductor superlattices could provide a new way of modulating energy band structures. They found a dramatic change in the electronic properties by adjusting the weight and the position of the defects in the barrier region. One of the noble features thus observed is that the miniband widths can be enhanced by several orders of magnitude especially when the energy level of the defect matches to the ground state of the corresponding isolated quantum well. More recent calculations done by Arsenault and Meunier² partially explain its physical origin. They proved through the study of resonant-tunneling time that the resonant energy of a δ -doped barrier has the larger width than that of an identical double-barrier structure.

In this communication, we present calculations showing that a periodic introduction of (either positive or negative) δ -function-like doping profiles in the well layers rather than the barrier layers provides another type of noble miniband modulations in semiconductor superlattices. We also provide the analytic formula for the energy dispersion relation extending the calculations of Beltram and Capasso.¹ The technique for atomic layer doping, δ -doping, is currently the subject of numerous experimental studies because it can provide very high electronic sheet densities with enhanced low-field mobility in compound semiconductors.³⁻⁵ For a GaAs/Ga_{1-x}Al_xAs heterostructure as an example, Si or Be sources⁶⁻⁸ can be used for such doping layers. We adopt here a δ -function model for such defects, either negative or positive depending on sources, since only their symmetry and weight are important, as discussed by Beltram and Capasso.¹ Such δ -function-like doping distributions can be achieved if dopants are spatially localized on the length scale of the lattice constant.

The main findings of the present study are depicted in Figs. 1 and 2. Figure 1(a) sketches the periodic structure with two conduction bands. When we introduce deep

levels in the center of well regions, shown as vertical lines in Fig. 1(b), the ground-state miniband shifts downwards, while the second band remains the same. As the weight of the defects increases, the ground-state miniband disappears as in Fig. 1(c) and only one band exists

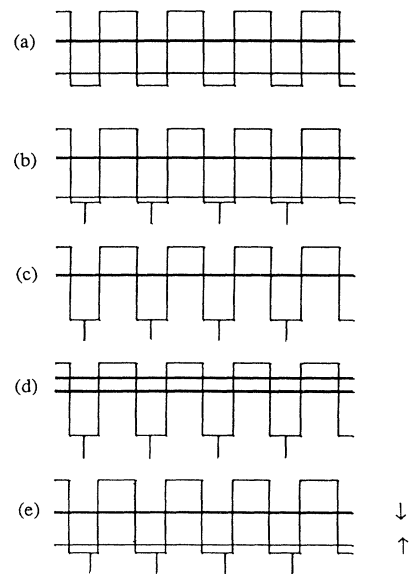


FIG. 1. Energy-band diagrams of a superlattice (a) without defects and (b)–(d) with defects (presented as negative δ potentials) in the middle of the wells in the order of increasing the weight. There is no change in the second band in (b)–(d). However, the first band shifts downwards (b) and finally disappears (c), and another band shows up above the second band (d). In (e) with the weight of defects the same as (b) but the defects are displaced from the central position: the first band shifts upward while the second shifts downward.

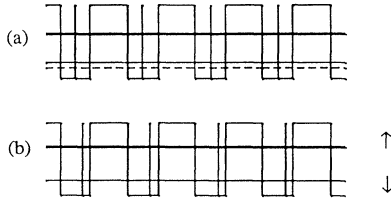


FIG. 2. Energy-band diagrams of a superlattice with defects, this time presented as positive δ potentials. In (a) the defects are in the middle of the wells. The first band shifts upward while the second remains unchanged. The dashed line presents the first band without defects. In (b) conditions are the same as (a) except that the defects are displaced from the central position. Compared to (a), the first band shifts upward while the second shifts downward.

in the structure. However, there is no noticeable change in the bandwidths. Further increase of the weight of the defects brings another band down to the structure coming from the continuum state, as shown in Fig. 1(d). When two bands in Fig. 1(d) match together (by adjusting the weight of the defects), the whole band structure looks like Fig. 1(c) but it splits into two narrow bands around the same band energy. For a GaAs/Ga_{0.7}Al_{0.3}As periodic structure with $w=80$ Å and $b=100$ Å, two bands without defects are centered at $E_0=42.5$ meV and $E_1=165.4$ meV with bandwidths $\Delta E_0=4.4 \times 10^{-2}$ meV and $\Delta E_1=1.1$ meV.⁹ Above w and b are thicknesses corresponding to the well and barrier layers, respectively. At matching conditions for two bands in Fig. 1(d), the E_1

band splits into two bands centered at 164.9 and 166.0 meV with equal widths of 0.1 meV. In addition to these noble features, variations in the position of the defect layer provide another degree of freedom in modulating the band structure. Figure 1(e) shows the case of Fig. 1(b), but with the defect layer displaced considerably from the center position in the well. Displacement of the defect layer from the center causes the E_0 band to move up but the E_1 band to move down (as indicated by arrows in the figure) so that the two bands become closer than in the case of Fig. 1(b).

Now, let us look at Fig. 2, which represents the periodic structure with positive δ potentials in the well; for example, Be dopants in GaAs layers. The general behavior here is completely opposite to earlier behavior. When the defects (with positive weights) are at the center of the well, the E_1 band remains the same but the E_0 band shifts upward, in contrast to Fig. 1(b). As defects move away from the center, the two bands get apart from each other, in contrast to Fig. 1(e). The schematic views shown in Figs. 1 and 2, together with the early findings by Beltram and Capasso,¹ suggest that one can control the band structure of superlattices in a diverse way by the introduction of periodic δ -doping layers.

The band-structure calculation of our proposed structure is similar to that of Beltram and Capasso.¹ It is performed via a Kane-type formalism¹⁰ using Bastard's boundary conditions,¹¹ which take into account the position-dependent effective mass. The effects of the defect are described via the δ function at the doping site. The dispersion relation between the Bloch wave vector k and the energy E (referred to the bottom of the well) can be written in an analytic form:

$$\cos(ka) = \cos(k_1 w) \cos(k_2 b) - \frac{(k_1/m_1^*)^2 + (k_2/m_2^*)^2}{2(k_1/m_1^*)(k_2/m_2^*)} \sin(k_1 w) \sin(k_2 b) \\ + \frac{m_1^* Q}{\hbar^2 k_1} \left\{ \sin(k_1 w) \cos(k_2 b) + \frac{\sin(k_1 w)}{(k_1/m_1^*)(k_2/m_2^*)} \left[\left[\frac{k_1}{m_1^*} \right]^2 \cos \left[\frac{k_1(w+2r)}{2} \right] \cos \left[\frac{k_1(w-2r)}{2} \right] \right. \right. \\ \left. \left. - \left[\frac{k_2}{m_2^*} \right]^2 \sin \left[\frac{k_1(w+2r)}{2} \right] \sin \left[\frac{k_1(w-2r)}{2} \right] \right] \right\}, \quad (1)$$

where Q and r are the weight and the position (from the center of the well) of the δ function, respectively, m_1^* , w and m_2^* , b are effective masses and thicknesses corresponding to the well and barrier layers, respectively, $a = w + b$ is the superlattice period, and k_1 and k_2 are the wave numbers in the wells and barriers given by

$$k_1 = \frac{(2m_1^* E)^{1/2}}{\hbar}, \quad k_2 = \frac{[2m_2^* (E - \Delta E_c)]^{1/2}}{\hbar}. \quad (2)$$

As expected, Eq. (1) returns to a simple Kronig-Penney model when $\Delta E_c = 0$ and $m_1^* = m_2^*$. The more general solution for the case of additional (periodic) defects in the barrier region can be written as

$\cos(ka) = \text{rhs of Eq. (1)}$

$$+ \frac{m_2^* P}{\hbar^2 k_2} \left\{ \cos(k_1 w) \sin(k_2 b) + \frac{\sin(k_1 w)}{(k_1/m_1^*)(k_2/m_2^*)} \left[\left(\frac{k_2}{m_2^*} \right)^2 \cos \left[k_2 \frac{b+2s}{2} \right] \cos \left[k_2 \frac{b-2s}{2} \right] - \left(\frac{k_1}{m_1^*} \right)^2 \sin \left[k_2 \frac{b+2s}{2} \right] \sin \left[k_2 \frac{b-2s}{2} \right] \right] \right\}, \quad (3)$$

where P and s are the weight and the position (from the center of the barrier) of the δ function introduced in the barrier layers.

Although Eq. (1) is in a compact form, it is not easy to see the overall picture shown in Figs. 1 and 2. In order to understand the role of defect layers rather easily, we consider an eigenvalue problem of a δ -doped single quantum well, as shown in Fig. 3, where the δ function locates at the center of the well (for simplicity). Due to the symmetry of the potential, we have even and odd solutions that satisfy the following relations:¹²

$$\tan \left[\frac{k_1 w}{2} \right] = \frac{2\kappa/\gamma + \bar{Q}}{2k_1 - \bar{Q}\kappa/\gamma k_1} \quad \text{even}, \quad (4)$$

$$\cot \left[\frac{k_1 w}{2} \right] = -\frac{\kappa}{k_1 \gamma} \quad \text{odd}, \quad (5)$$

where $\bar{Q} = 2Qm_1^*/\hbar^2$, $\gamma = m_2^*/m_1^*$, and $\kappa = -ik_2$. The odd solutions are not affected by the defects because the wave function becomes a node at the center of the well. This explains why the second band, E_1 remains unchanged in Figs. 1 and 2 for defects located at the center of the well layers. However, the even solutions are strongly affected by the value of \bar{Q} . Increasing \bar{Q} with the positive value always increases the even-state eigenvalues, which, however, have the certain limit

$$k_1 w = 2 \tan^{-1}(-\gamma k_1/\kappa) + 2n\pi \quad \text{for } \bar{Q} \rightarrow \infty \quad \text{even} \\ (n = 1, 2, 3, \dots) \quad (6)$$

where the values of the inverse tangent are taken between

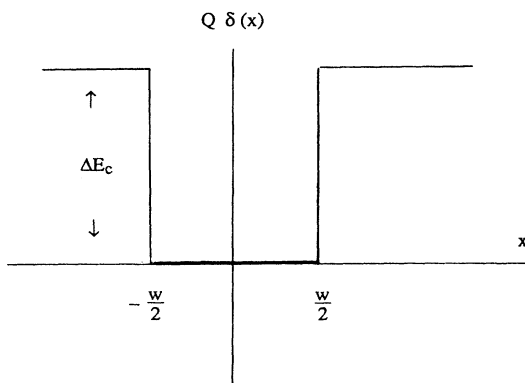


FIG. 3. δ -doped single quantum well.

$-\pi/2$ and 0. For $\bar{Q} < 0$, the situation is rather complicated. As the magnitude of \bar{Q} increases (with the negative value), the ground-state energy decreases and finally vanishes, and the next order solution will be the lowest possible one at this time which is

$$k_1 w = 2 \tan^{-1} \left[\frac{2\kappa/\gamma + \bar{Q}}{2k_1 - \bar{Q}\kappa/\gamma k_1} \right] + 2\pi, \quad (7)$$

where the values of inverse tangent are taken between $-\pi/2$ and 0 (the argument in parentheses is less than 0 in this case). These observations are very consistent with

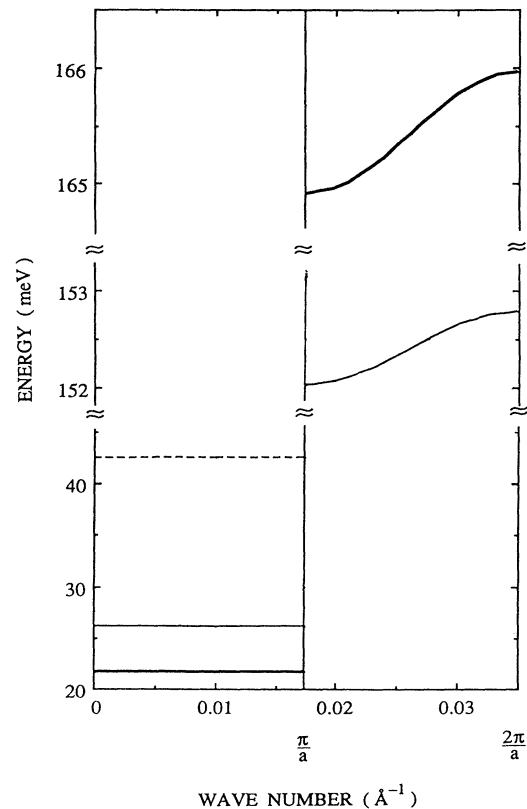


FIG. 4. Energy dispersion relation in the extended zone scheme for a GaAs/Ga_{0.7}Al_{0.3}As superlattice. Dashed, thick solid, and thin solid lines correspond to the case of Figs. 1(a), 1(b), and 1(e), respectively. In the second zone, the dashed line completely overlaps with the thick solid line. Detailed parameters are given in the text.

the behavior shown in Figs. 1(b)–1(d). The matching condition for the two bands appearing in Fig. 1(d) is exactly the same as matching Eq. (7) with the lowest odd solution in Eq. (5). Under such circumstances, the actual band splits into two narrow bands around E_1 , as mentioned earlier. This kind of energy splitting is similar to what happens in the usual band-structure calculations, i.e., the degeneracy can be broken when the off-diagonal matrix element is nonzero.¹³ Figure 4 shows the energy dispersion relation with and without deep levels in the well for an 80-Å well, 100-Å barrier GaAs/Ga_{0.7}Al_{0.3}As superlattice.⁹ For the weight of the defects, $\bar{Q} = -0.01$ a.u. is used in the figure. The effect of a displacement r of the defect (from the central position in the well) is clearly shown as a thin solid curve for $r = 20$ Å. It is worth

mentioning that the width of the first band ($= 4.4 \times 10^{-2}$ meV) remains the same in all cases despite changes in the band energy.

In conclusion, we have shown that superlattice band structure can be greatly modified by introducing δ -doping layers in the well layers as well as in the barrier layers of a superlattice. Together with the work of Beltram and Capasso,¹ we are able to design superlattices in a diverse way; the control on the band gap, the position of the energy bands and their width, the creation of a new band, and the annihilation of the existing band, etc.

This work is supported by the Ministry of Science and Technology, Korea.

¹F. Beltram and F. Capasso, *Phys. Rev. B* **38**, 3580 (1988).

²C. J. Arsenault and M. Meunier, *Phys. Rev. B* **39**, 8739 (1989).

³E. F. Schubert, J. E. Cunningham, and W. T. Tsang, *Solid State Commun.* **63**, 591 (1987).

⁴A. Zrenner, F. Koch, and K. Ploog, *Inst. Phys. Conf. Ser.* **91**, 171 (1988).

⁵W. Cheng, A. Zrenner, Q. Ye, F. Koch, D. Grutzmacher, and P. Balk, *Semicond. Sci. Technol.* **4**, 16 (1989).

⁶E. F. Schubert, J. B. Stark, B. Ullrich, and J. E. Cunningham, *Appl. Phys. Lett.* **52**, 1508 (1988).

⁷E. F. Schubert, C. W. Tu, R. F. Kopf, J. M. Kuo, and L. M. Lunardi, *Appl. Phys. Lett.* **54**, 2592 (1989).

⁸E. F. Schubert, J. M. Kuo, R. F. Kopf, H. S. Luftman, L. C.

Hopkins, and N. J. Sauer, *J. Appl. Phys.* **67**, 1969 (1990).

⁹We assumed the following material parameters: $\Delta E_c = 271$ meV, $m^* = 0.096m_0$ in the Ga_{0.7}Al_{0.3}As barrier layer, and $m^* = 0.067m_0$ in the GaAs well layer. ΔE_c is the conduction-band offset.

¹⁰E. O. Kane, *J. Phys. Chem. Solids* **1**, 249 (1957).

¹¹G. Bastard, *Phys. Rev. B* **24**, 5693 (1981).

¹²The same notations as in Eq. (1) are used. γ will be 1 if there is no effective-mass difference between the well and the infinite barrier.

¹³For example, see N. W. Ashcroft and N. D. Mermin, *Solid State Physics* (Holt, Rinehart and Winston, New York, 1976), Chap. 9.